THE JOURNAL OF PHYSICAL CHEMISTRY C

ARTICLE

pubs.acs.org/JPCC

Switching, Dual Spin-Filtering Effects, and Negative Differential Resistance in a Carbon-Based Molecular Device

Haiqing Wan,[†,‡] Benhu Zhou,[†] Xiongwen Chen,[†] Chang Q. Sun,[§] and Guanghui Zhou*[,†,∥]

[†]Department of Physics and Key Laboratory for Low-Dimensional Quantum Structures and Manipulation (Ministry of Education), Hunan Normal University, Changsha 410081, China

[‡]Department of Science, Nanchang Teachers College, Nanchang 330029, China

[§]School of Electrical and Electronic Engineering, Nanyang Technological University, Singapore 639798, Singapore

[∥]International Center for Materials Physics, Chinese Academy of Sciences, Shenyang 110015, China

ABSTRACT: We present ab initio calculations for spin-dependent electron transport in a molecular device constructed by two carbon chains capped with a phenyl ring, which is sandwiched between two zig-zag-edged graphene nanoribbon (ZGNR) electrodes, where the ZGNRs are modulated by external magnetic field. The coexistence of switching, dual spin-filtering effects, and negative differential resistance (NDR) in the model device is demonstrated with the theory of carbon π-electrons. Interestingly, a two-state molecular conformational switch can be realized by changing the orientation between the planes of phenyl ring and electrodes, where the majority-spin current modulation (ON/OFF ratio) is 170−479 within the considered bias window. Moreover, the device shows perfect dual spin-filtering effect and can generate and control a full dual spin-polarized current through either the source-drain voltage or magnetic configuration of the electrodes. The selective spin current is due to a dual selection rule, the symmetry match between two ZGNR electrodes spin channel, and the carbon chain's spin selection in our system. In addition, the obvious NDR behavior has also been observed in our model.

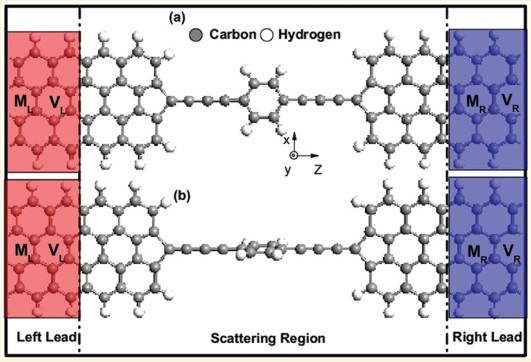

I. INTRODUCTION

In recent years, much effort has been devoted experimentally[1−4] and theoretically[5−11] to various molecular electronic devices. In particular, mechanically controlled switches containing organic molecules have been an interesting topic for the possibility of electron-transport manipulation by changing molecular conformation. It was previously demonstrated[5,6] that the conduction of a molecular wire containing phenyl rings is strongly influenced by the molecular conformation. Later, the switching behavior by conformational change in a $\pi-\sigma-\pi$ molecular wire has been investigated.[7] Molecular conductivity switching of two benzene rings based on torsion-angle conformation variation driven by a gate electric field has been recently shown.[8] Moreover, a highly efficient switch built from an organic molecule assembled between single-wall carbon nanotube electrodes has been recently proposed[9] and observed.[1−4] Meanwhile, the negative differential resistance (NDR) phenomenon in molecular conductors also has gained widespread interest because of potential applications including amplification, logic, memory, and so on. NDR effect can be found in a variety of molecular devices, such as Si nanowire,[12] a Au/S-azobenzene-S/Au wire,[13] Al/carbon-nanotube/Al junctions,[14] or the Au/AN-OPE/RS/Hg self-assembled monolayer system.[15]

Moreover, because graphene[16] and graphene nanoribbons (GNRs)[17] were fabricated, they have been proposed as electrodes in spintronics devices for spin injection.[18] In addition, single carbon atomic chain can be an important component in molecular devices,[19,20] and it has been directly carved out from graphene in recent experiments.[21−23] Consequently, the spin-dependent transport for carbon chains between GNRs has been triggered a massive interest.[24−29] Carbon atomic chains as spin-transmitters[24,25] have been studied. Furthermore, the possibility for controlling carbon chain conductance, optical properties, and spin magnetization, purely by twisting its sp^2 termination, has been demonstrated.[28] Moreover, carbon-chain-bridging GNR electrodes as a good spin-filter or spin-valve has been proposed by Zeng et al.[29] recently. However, the pure carbon-based spintronics molecular device with the coexistence of switching, NDR, and spin-filtering effects has not been previously reported.

In this Article, we numerically investigate the spin-resolved electron transport for a molecular device constructed by two carbon chains capped with a phenyl ring, which is sandwiched between two ferromagnetic zig-zag-edged GNR (ZGNR) electrodes. In ZGNR,

Received: September 25, 2011
Revised: December 22, 2011
Published: December 22, 2011

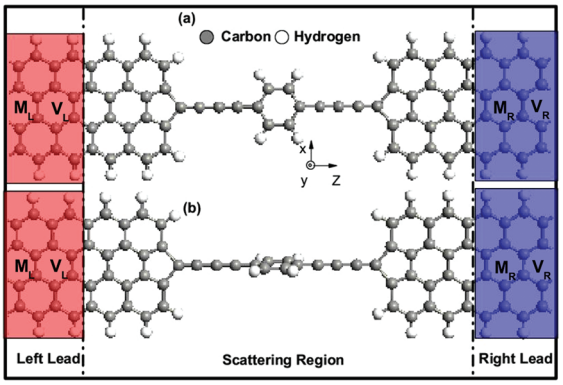

Figure 1. Schematic of the model device with (a) coplanar and (b) perpendicular conformation between planes of phenyl ring and ZGNR electrodes, where the shaded areas of ZGNR electrodes are modulated by an external magnetic field, within which results in magnetization on left electrode (M_L) and right electrode (M_R). The value of either M_L or M_R can be 1, or −1, which corresponds to the magnetization along the $+y$ and $-y$ direction, respectively. The difference in the electrostatic potentials between the electrodes leads to a bias voltage ($V = V_L - V_R$), which generates a current.

magnetic exchange interactions between the spin states at the edges favor antiparallel (antiferromagnetic) configurations. However, in the presence of a suitable magnetic modulation, the ZGNR with parallel (ferromagnetic) edge states could be more stable.[30,31] Moreover, ferromagnetic ZGNRs are metallic, but antiferromagnetic ones are semiconducting.[32,33] Therefore, the external magnetic field on ZGNRs makes the electrodes provide spin-polarized electrons and electrostatic potentials under a suitable bias voltage. Interestingly, we have observed a maximum ON/OFF ratio of 479/550 for majority-spin (α)/minority-spin (β) state by changing the orientation between planes of phenyl ring and ZGNRs. Moreover, the device shows a perfect dual spin-filtering effect, and a full spin-polarized current can be generated and controlled through either the source-drain voltage or magnetic configuration of the electrodes. The selective spin current is attributed to the dual selection rule, symmetry match between two ZGNR electrode spin channels, and the carbon chain's spin selection in our system, which is different from pure ZGNR junction in antiferromagnetic.[34] In addition, the obvious NDR behavior can be realized in our model. These results indicate that our proposed device has a wide range of applications, including molecular switching, logic and memory, as well as bipolar spin diodes.

II. MODEL AND METHOD

The model device is illustrated in Figure 1, where the two orientations of coplanar and perpendicular between phenyl ring and ZGNRs are considered. An external magnetic field controls the magnetization of the left (right) ZGNR electrode denoted as M_L (M_R), which can be set to 1 or −1, which corresponds to the magnetization along the $+y$ or $-y$ direction. If the magnetic fields at two electrodes point in the same or opposite direction, that is, (M_L, M_R) = (1,1) or (1,−1), then the ZGNR electrodes would show the parallel (P) or antiparallel (AP) spin configuration. An N-ZGNR has number of N zig-zag carbon chains along its width.[32] We focus on the case of 4-ZGNR electrode because only the ZGNRs with an even number of chains exhibits dual spin-filtering effect due to the symmetry of ZGNRs.[34] In addition, the carbon

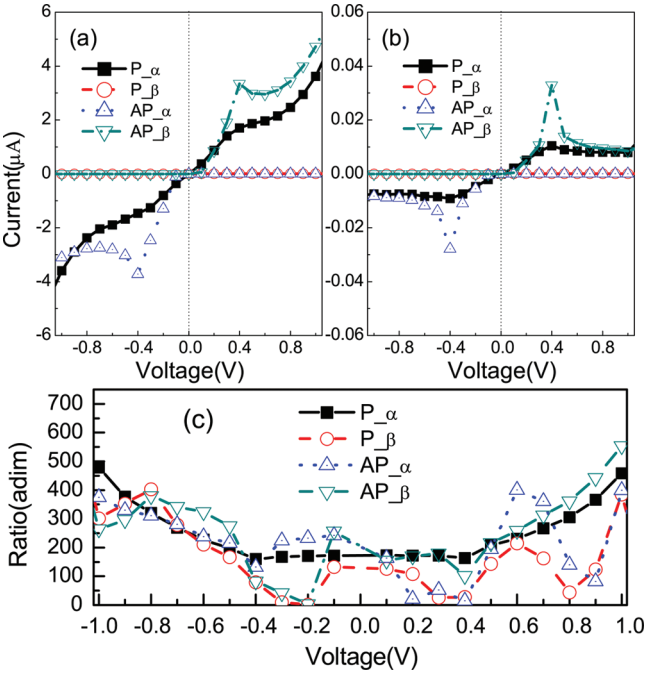

Figure 2. Spin-resolved $I-V$ curves for two different phenyl ring conformations with respect to ZGNRs, where (a) ON state corresponds to the coplanar conformation and (b) OFF state to the perpendicular conformation. Panel c shows ON/OFF switch ratios.

chain structures in scattering region are of the double-bonded or alternating single-triple bonded, which is dependent on the even or odd number of carbon atoms.[35−37] So the carbon chains can be directly capped with phenyl ring, which makes them much more stable and easier to manipulate,[38] and the reversible orientation transitions between phenyl ring and ZGNRs may be realized by thermal activation, micromechanical operation, or electric field.[8−11]

The geometric optimization and spin-resolved electron transport properties are calculated by a developed ab initio software package Atomistix ToolKit,[39,40] which is based on the spin-polarized density-functional theory combined with the nonequilibrium Greens functions. In the calculation, the local-density approximation for exchange-correlation potential, k-point grid $1 \times 1 \times 100$, norm-conserving pseudopotentials are used, and the convergence criterion for Hamiltonian and the electron density are 10^{-5} in total energy. The geometry optimization is performed for the scattering region using quasi-Newton method until the absolute value of force acting on each atom is <0.05 eV/Å. ZGNRs connected to the carbon chain through a five-membered ring.[22] The spin-resolved current is calculated using the Landauer−Büttiker formula[7,10,20,29]

$$I_\sigma(V) = (e/h)\int_{\mu_L}^{\mu_R} T_\sigma(E,V)[f_L(E-\mu_L) - f_R(E-\mu_R)]\,dE \quad (1)$$

where $\mu_{L/R}$ is the electrochemical potential of the left/right electrode, $T_\sigma(E, V)$ is the spin-resolved transmission probability with energy E and bias voltage V, and $f_{L/R}(E) = 1/[1 + \exp((E - \mu_{L/R})/K_BT)]$ is the Fermi−Dirac distribution function.

III. RESULTS AND DISCUSSION

Figure 2 shows the calculated spin-resolved current−voltage ($I-V$) cuvre for the device with different phenyl ring

dx.doi.org/10.1021/jp2092576 |J. Phys. Chem. C 2012, 116, 2570–2574

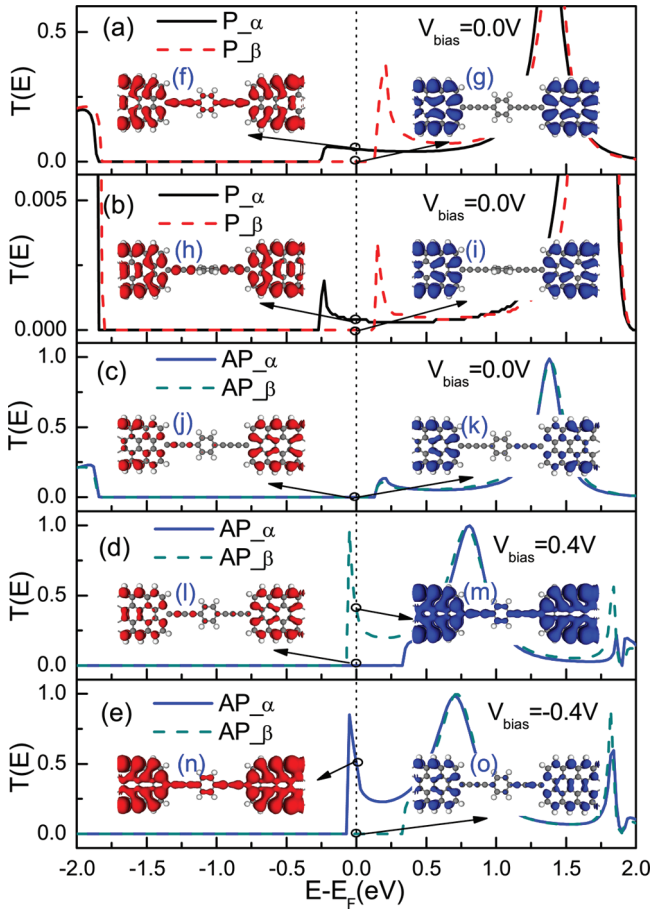

Figure 3. Spin-resolved transmission for different spins under various bias and electrode magnetic configurations. (a,b) Coplanar/perpendicular phenyl ring conformation with PSOE under zero bias. (c−e) Under bias of 0, 0.4, and −0.4 V for coplanar conformation with APSOE. Inset: spin-resolved LDOS at E_F, (f,g) for coplanar and (h,i) for perpendicular conformation with PSOE under zero bias and (j−o) for coplanar conformation with APSOE under bias of 0, 0.4, and −0.4 V.

conformations with respect to electrodes and spin orientation of electrodes within the bias range (−1, 1 V). For coplanar conformation as shown in Figure 2a, the α current with parallel spin orientation of electrodes (PSOE) (P_α) shows linear and nonlinear $I-V$ characteristics with small and large (>0.35 V) bias, respectively, whereas the β current with PSOE (P_β) is blocked in the whole bias range, the device shows perfect spin-filtering effect in PSOE case. Interestingly, a perfect dual spin diode effect appears in the case of anti-PSOE (APSOE). The α/β current with APSOE (AP_α/AP_β) under a negative bias is completely opposite to that under a positive bias. The electron of AP_α/AP_β substantially flows only in the negative/positive bias range, whereas it blocks in the positive/negative bias range. The ratio of the spin-dependent current, AP_α/AP_β, can be up to 1.8×10^4 at −0.4 V, which is equivalent to the rectification ratio for each spin-dependent current, and the value is much larger than that in previous study.[34] Therefore, the unidirectional spin-polarized current can be selectively generated and controlled by the source-drain voltage. Meanwhile, the device also shows a NDR behavior at bias ±0.4 V in APSOE case. In contrast, for perpendicular conformation as shown in Figure 2b, the values for AP_α and AP_β are negligibly small (lower than 0.03 μA), but they show more visible NDR. (The peak-to-valley ratio is increased to 3.37 from 1.36.) NDR is very important in the field of electronic technology due to lots of applications in the area of semiconductor physics, and it can be experimentally observed in some physical systems.[41] We also see that the phenyl ring conformation plays an important switching role, as is shown in Figure 2c, where the ON/OFF switch ratios between coplanar and perpendicular conformation states are presented for the device within the considered bias range. In particular, although the ON/OFF ratio at large bias can be up to 550 for P_β, it shows a 170 plateau in bias range (−0.4, 0.4 V) and reaches a maximum value of 479 at large bias for P_α. This effect provides a good switch function by controlling the phenyl ring conformation.

To explain the above $I-V$ characteristics, in Figure 3, we present the spin-resolved transmission associated with local density of states (LDOS) around the Fermi level (E_F). The spin orientation of the electrodes in Figures 3a,b is parallel, whereas that in Figure 3c−e is antiparallel. As shown in Figure 3a,b, although the phenyl ring conformation with respect to electrodes does not affect qualitatively the transmission behavior, the value of transmission for the case of coplanar conformation (Figure 3a) is much greater than that in the perpendicular case (Figure 3b), which results in the switching effect for the device. Furthermore, the transport mechanism originates from the difference in LDOS around E_F between two conformation cases. As shown in Figure 3a [inset (d)], the (red) π-orbital amplitude is on all carbon atoms of the atomic chain and phenyl ring in the case of coplanar conformation. However, the (red) cloud is only alternatively localized on the carbon atoms of chain in the perpendicular conformation case, as shown in Figure 3b [inset (f)]. This is because only the p_y channel of carbon chain overlaps with the delocalized big π-orbital of graphene, and thus it contributes to the conductance. When the overlap of the carbon chain's p_y channel and the phenyl ring's π-orbital takes a maximum value in the coplanar conformation case, p_y channel is fully open and π-electrons can easily go through the phenyl ring. Whereas the overlap takes a minimum value in the perpendicular conformation case, p_y channel is localized and π-electrons can hardly go through phenyl ring.[5,7,42] Therefore, the transmission in perpendicular conformation case is negligibly small. From Figure 3a,b, one find the full spin-polarization around E_F in both coplanar and perpendicular conformation cases at zero bias with PSOE. The transmission spin-polarization, defined[18,24,29] by TSP = $(T_\alpha - T_\beta)/(T_\alpha + T_\beta) \times 100$, approaches 100% in both cases. This result is supported by the spin-resolved LDOS at E_F shown in insets f−i in Figure 3a,b. The α-state electrons are transported at E_F, but β-state electrons are blocked. This is because of spin-selective transmission with the carbon chain's orbital matching to source ZGNR leads. To understand the perfect dual spin-polarization that appeared in the APSOE case, we plotted the spin-dependent transmission spectrum at bias of 0, 0.4, and −0.4 V for coplanar conformation with APSOE in Figure 3c−e. As shown in Figure 3c, although the electron spin is not resolved between α and β states at zero bias and both α and β channels are blocked at the Fermi level, the β/α transmission shift toward the Fermi level as bias increases to the positive/negative direction, as illustrated in Figure 3d,e. This lead to the β/α-state electrons being only transported under a positive/negative bias but insulated under a negative/positive bias. In recent works,[34,43] the selective spin current through an antiferromagnetic junction of symmetric ZGNR is attributed to the orbital symmetry of spin subbands. However, the mechanism of selective transmission in

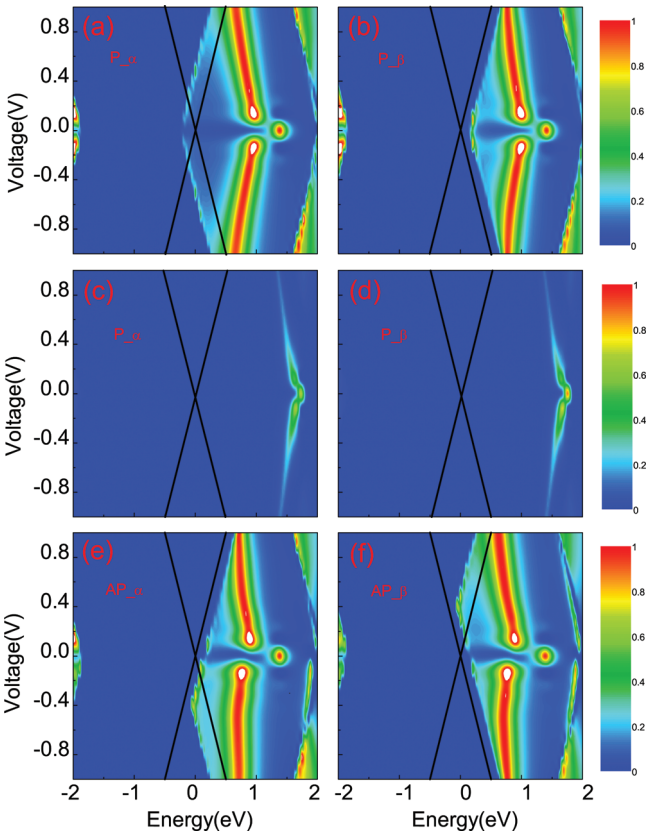

Figure 4. Spin-resolved transmission as a function of electron energy and bias, where (a,b) corresponds to α/β for coplanar conformation with PSOE, (c,d) corresponds to α/β for perpendicular conformation with PSOE, and (e,f) corresponds to α/β for coplanar conformation with APSOE. The (black) cross line region is referred to the bias window.

our system is different due to a dual selection rule, that is, symmetry match for the spin channel between the two ZGNR electrodes and the carbon chain's spin selection. On one hand, a positive/negative bias shifts the energy bands of the left and right electrodes, which lead to the symmetry match of β/α subbands and mismatch of the α/β subbands. So, the β/α channel is opened, whereas the α/β channel is closed. On the other hand, the carbon chain also has spin selection and only allow the transmission of one spin channel of source electrode. It can also be verified from the spin-resolved LDOS at E_F, as shown in insets l−o of Figure 3d,e. The β-state electrons of source electrode are transported at E_F, but the α-state electrons of drain electrode are blocked in the positive bias range, which is opposite in contrast with that in the negative bias range.

Also, to understand further the $I-V$ characteristics, Figure 4 plots the spin-resolved transmission as a function of both electron energy and bias. Figure 4a,b corresponds to α/β transmission for coplanar conformation with PSOE, Figure 4c, d corresponds to that for perpendicular conformation with PSOE, whereas Figure 4e,f corresponds to that for coplanar conformation with APSOE. From the Landauer−Büttiker formula, we know that the spin-resolved current through central scattering region is decided by the transmission within the considered bias window. By comparing Figure 4a,b, one observes that fairly big α transmission for coplanar conformation with PSOE occurs within the bias (−1, 1 V) shown by (black) cross line, whereas β transmission is shifted away from this window.

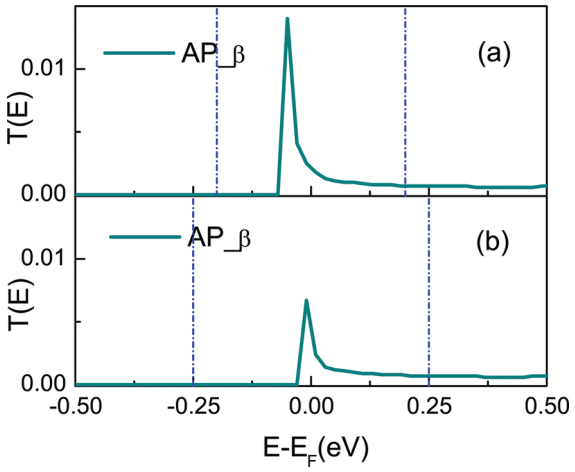

Figure 5. Spin-resolved transmission (solid lines) for perpendicular conformation under the biases V = 0.4 and 0.5 V with APSOE. The region between the dashed-dotted lines is the bias window.

This phenomenon leads to a significant difference in current between two spin states, as shown by P_α and P_β in Figure 2a, which indicates perfect spin-filtering effect. For perpendicular conformation, as described in Figures 4c,d, however, the transmission is negligibly small within the bias window. As a result, the spin-resolved current is much smaller than that of coplanar conformation, which leads to the switching behavior. For coplanar conformation with APSOE, as can be seen in Figure 4e,f, the α/β transmission within the bias window is always zero under a positive/negative bias. Therefore, the α/β current is always suppressed under the positive/negative bias. On the contrary, the α/β transmission shifts into the bias window under a negative/positive bias, resulting in a increasing current. As a result, a perfect dual spin filter exhibits in APSOE.

Finally, it is known that in the context of molecular electronics there are various types of mechanisms that can lead to the phenomenon of NDR. One of them is the conduction orbital being suppressed at a certain bias voltage.[14] To understand clearly the NDR behavior in our model, in Figure 5a,b, we give the β-transmission coefficients with APSOE at two special bias voltages of 0.4 and 0.5 V for perpendicular conformation, respectively. We know that the current is determined only by the integral area in the bias window. From Figure 4a, we can find that when the bias voltage is 0.4 V, there is a large transmission peak in the bias window, which leads to a large current. However, when the bias takes the value 0.5 V, it can be found from Figure 4b that the bias window increases with the bias voltage, but the corresponding transmission coefficient and the total integral area gets smaller, which means that the corresponding orbital is suppressed. As a result, the current decreases and the NDR appears.

IV. SUMMARY

In summary, we have proposed a molecular device with coexistence of switching, NDR, and dual spin-filtering functions. It is constructed by two carbon chains capped with a phenyl ring between two ferromagnetic ZGNR electrodes. Our results show that a two-state molecular conformational switch can be realized by mechanically changing the orientation between the planes of phenyl ring and ZGNRs, and the modeled device exhibits

substantially large current modulation (ON/OFF ratio). Moreover, the device shows perfect dual spin-filtering effect and can generate and control a full spin-polarized current through either the source-drain voltage or magnetic configuration of electrodes. The selective spin current is due to a dual selection rule, that is, symmetry match between two ZGNR electrodes spin channel and the carbon chain's spin selection, which has different selection mechanism. The device also shows an obvious NDR behavior. Therefore, it reveals the potential of usage as molecular switching, logic, and memory as well as effective bipolar spin diodes.

AUTHOR INFORMATION

Corresponding Author
*E-mail: ghzhou@hunnu.edu.cn.

ACKNOWLEDGMENT

This work was supported by the National Natural Science Foundation of China (grant no. 10974052), the Program for Changjiang Scholars and Innovative Research Team in University (PCSIRT, No. IRT0964), the Hunan Provincial Natural Science Foundation of China (grant No. 11JJ7001), the Scientific Research Fund of Jiangxi Provincial Education Department (Grant No. GJJ11647), and Hunan Provincial Innovation Foundation for Postgraduate (Grant No. CX2011B186).

REFERENCES

(1) Ramachandran, K. G.; Hopson, T. J.; Rawlett, A. M.; Nagahara, L. A.; Primak, A.; Lindsay, S. M. *Science* **2003**, *300*, 1413–1416.
(2) Comstock, M. J.; Levy, N.; Kirakosian, A.; Cho, J.; Lauterwasser, F.; Harvey, J. H.; Strubbe, . A.; Fréchet, J. M. J.; Trauner, D.; Louie, S. G.; Crommie, M. F. *Phys. Rev. Lett.* **2007**, *99*, 038301.
(3) Liu, C. L.; Kurosawa, T.; Yu, A. D.; Higashihara, T.; Ueda, M.; Chen, W. C. *J. Phys. Chem. C* **2011**, *115*, 5930–5939.
(4) Malic, E.; Weber, C.; Richter, M.; Atalla, V.; Klamroth, T.; Saalfrank, P.; Reich, S.; Knorr, A. *Phys. Rev. Lett.* **2011**, *106*, 097401.
(5) Samanta, M. P.; Tian, W.; Datta, S.; Henderson, J. I.; C. Kubiak, P. *Phys. Rev. B* **1996**, *53*, R7626–R7629.
(6) Magoga, M.; Joachim, C. *Phys. Rev. B* **1999**, *59*, 16011–16021.
(7) Pati, R.; Karna, S. P. *Phys. Rev. B* **2004**, *69*, 155419.
(8) Vergniory, M. G.; Granadino-Roldan, J. M.; Garcia-Lekue, A.; Wang, L. W. *Appl. Phys. Lett.* **2010**, *97*, 262114.
(9) Martins, T. B.; Fazzio, A.; da Silva, A. J. R. *Phys. Rev. B* **2009**, *79*, 115413.
(10) Qiu, M.; Zhang, Z. H.; Deng, X. Q.; Chen, K. Q. *J. Appl. Phys.* **2010**, *107*, 063704.
(11) Taylor, J.; Brandbyge, M.; Stokbro, K. *Phys. Rev. B* **2003**, *68*, 121101.
(12) Dong, J. C.; Li, H.; Sun, F. W.; Zhang, K.; Li, Y. F. *J. Phys. Chem. C* **2011**, *115*, 13901–13906.
(13) Zhang, C.; He, Y.; Cheng, H. P.; Xue, Y.; Ratner, M. A.; Zhang, X. G.; Krstic, P. *Phys. Rev. B* **2006**, *73*, 125445.
(14) Li, X. F.; Chen, K. Q.; Wang, L. L.; Long, M. Q.; Zou, B. S.; Shuai, Z. *Appl. Phys. Lett.* **2007**, *91*, 133511.
(15) Kim, H.; Jang, S. S.; Kiehl, R. A.; Goddard, W. A. *J. Phys. Chem. C* **2011**, *115*, 3722–3730.
(16) Novoselov, K. S.; Geim, A. K.; Morozov, S. V.; Jiang, D.; Zhang, Y.; Dubonos, S. V.; Grigorieva, I. V.; Firsov, A. A. *Science* **2004**, *306*, 666–669.
(17) Han, M. Y.; Özyilmaz, B.; Zhang, Y.; Kim, P. *Phys. Rev. Lett.* **2007**, *98*, 206805.
(18) Koleini, M.; Paulsson, M.; Brandbyge, M. *Phys. Rev. Lett.* **2007**, *98*, 197202.
(19) Lang, N. D.; Avouris, P. *Phys. Rev. Lett.* **1998**, *81*, 3515–3518.
(20) Larade, B.; Taylor, J.; Mehrez, H.; Guo, H. *Phys. Rev. B* **2001**, *64*, 075420.
(21) Meyer, J. C.; Girit, C. O.; Crommie, M. F.; Zettl, A. *Nature* **2008**, *454*, 319–322.
(22) Jin, C.; Lan, H. p.; Peng, L. m.; Suenaga, K.; Iijima, S. *Phys. Rev. Lett.* **2009**, *102*, 205501.
(23) Chuvilin, A.; Meyer, J. C.; Algara-Siller, G.; Kaiser, U. *New J. Phys.* **2009**, *11*, 083019.
(24) Fürst, J. A.; Brandbyge, M.; Jauho, A.-P. *Eur. Phys. Lett.* **2010**, *91*, 37002.
(25) Zanolli, Z.; Onida, G.; Charlier, J.-C. *ACS Nano* **2010**, *4*, 5174–5180.
(26) Zhang, G. P.; Fang, X. W.; Yao, Y. X.; Wang, C. Z.; Ding, Z. J.; Ho, K. M. *J. Phys.: Condens. Matter* **2011**, *23*, 025302.
(27) Chen, W.; Andreev, A. V.; Bertsch, G. F. *Phys. Rev. B* **2009**, *80*, 085410.
(28) Ravagnan, L.; Manini, N.; Cinquanta, E.; Onida, G.; Sangalli, D.; Motta, C.; Devetta, M.; Bordoni, A.; Piseri, P.; Milani, P. *Phys. Rev. Lett.* **2009**, *102*, 245502.
(29) Zeng, M. G.; Shen, L.; Cai, Y. Q.; Sha, Z. D.; Feng, Y. P. *Appl. Phys. Lett.* **2010**, *96*, 042104.
(30) Kim, W. Y.; Kim, K. S. *Nat. Nanotechnol.* **2008**, *3*, 408–412.
(31) Pisani, L.; Chan, J. A.; Montanari, B.; Harrison, N. M. *Phys. Rev. B* **2007**, *75*, 064418.
(32) Son, Y. W.; Cohen, M. L.; Louie, S. G. *Phys. Rev. Lett.* **2006**, *97*, 216803.
(33) Yang, L.; Park, C. H.; Son, Y. W.; Cohen, M. L.; Louie, S. G. *Phys. Rev. Lett.* **2007**, *99*, 186801.
(34) Ozaki, T.; Nishio, K.; Weng, H.; Kino, H. *Phys. Rev. B* **2010**, *81*, 075422.
(35) McCarthy, M. C.; Travers, M. J.; Kovacs, A.; Chen, W.; Novick, S. E.; Gottlieb, C. A.; Thaddeus, P. *Science* **1997**, *275*, 518–520.
(36) Bodart, V. P.; Delhalle, J.; Dory, M.; Fripiat, J. G.; Andre, J. M. *J. Opt. Soc. Am. B* **1987**, *4*, 1047–1054.
(37) Khoo, K. H.; Neaton, J. B.; Son, Y. W.; Cohen, M. L.; Louie, S. G. *Nano Lett.* **2008**, *8*, 2900–2905.
(38) Garcla-Suárez, V. M.; Lambert, C. J. *Nanotechnology* **2008**, *19*, 455203–455203.
(39) Brandbyge, M.; Mozos, J. L.; Ordejón, P.; Taylor, J.; Stokbro, K. *Phys. Rev. B* **2002**, *65*, 165401.
(40) Taylor, J.; Guo, H.; Wang, J. *Phys. Rev. B* **2001**, *63*, 121104(R).
(41) (a) Chen, J.; Reed, M. A.; Rawlett, A. M.; Tour, J. M. *Science* **1999**, *286*, 1550–1552. (b) Lyo, I.-W.; Avouris, P. *Science* **1989**, *245*, 1369–1371.
(42) Shen, L.; Zeng, M. G.; Yang, S. W.; Zhang, C.; Wang, X. F.; Feng, Y. P. *J. Am. Chem. Soc.* **2010**, *132*, 11481–11486.
(43) Zeng, M. G.; Shen, L.; Zhou, M.; Zhang, C.; Feng, Y. P. *Phys. Rev. B* **2011**, *83*, 115427.